

Published in final edited form as:

*Nitric Oxide*. 2014 February 15; 37: 41–45. doi:10.1016/j.niox.2013.12.010.

## Inhibition of xanthine oxidase by the aldehyde oxidase inhibitor raloxifene: Implications for identifying molybdopterin nitrite reductases

E.R. Weidert<sup>a,1</sup>, S.O. Schoenborn<sup>a,1</sup>, N. Cantu-Medellin<sup>a,b</sup>, K.V. Choughule<sup>c</sup>, J.P. Jones<sup>c</sup>, and E.E. Kelley<sup>a,b,\*</sup>

<sup>a</sup>University of Pittsburgh School of Medicine, Department of Anesthesiology, United States

<sup>b</sup>University of Pittsburgh School of Medicine, Vascular Medicine Institute, United States

<sup>c</sup>Washington State University, Department of Chemistry, United States

### Abstract

Sources of nitric oxide alternative to nitric oxide synthases are gaining significant traction as crucial mediators of vessel function under hypoxic inflammatory conditions. For example, capacity to catalyze the one electron reduction of nitrite ( $\text{NO}_2^-$ ) to  $\cdot\text{NO}$  has been reported for hemoglobin, myoglobin and molybdopterin-containing enzymes including xanthine oxidoreductase (XOR) and aldehyde oxidase (AO). For XOR and AO, use of selective inhibition strategies is therefore crucial when attempting to assign relative contributions to nitrite-mediated  $\cdot\text{NO}$  formation in cells and tissue. To this end, XOR inhibition has been accomplished with application of classic pyrazolopyrimidine-based inhibitors allo/oxypurinol or the newly FDA-approved XOR-specific inhibitor, Uloric<sup>®</sup> (febuxostat). Likewise, raloxifene, an estrogen receptor antagonist, has been identified as a potent ( $K_i = 1.0 \text{ nM}$ ) inhibitor of AO. Herein, we characterize the inhibition kinetics of raloxifene for XOR and describe the resultant effects on inhibiting XO-catalyzed  $\cdot\text{NO}$  formation. Exposure of purified XO to raloxifene (PBS, pH 7.4) resulted in a dose-dependent (12.5–100  $\mu\text{M}$ ) inhibition of xanthine oxidation to uric acid. Dixon plot analysis revealed a competitive inhibition process with a  $K_i = 13 \mu\text{M}$ . This inhibitory process was more effective under acidic pH; similar to values encountered under hypoxic/inflammatory conditions. In addition, raloxifene also inhibited anoxic XO-catalyzed reduction of  $\text{NO}_2^-$  to  $\cdot\text{NO}$  ( $\text{EC}_{50} = 64 \mu\text{M}$ ). In contrast to having no effect on XO-catalyzed uric acid production, the AO inhibitor menadione demonstrated potent inhibition of XO-catalyzed  $\text{NO}_2^-$  reduction ( $\text{EC}_{50} = 60 \text{ nM}$ ); somewhat similar to the XO-specific inhibitor, febuxostat ( $\text{EC}_{50} = 4 \text{ nM}$ ). Importantly, febuxostat was found to be a very poor inhibitor of human AO ( $\text{EC}_{50} = 613 \mu\text{M}$ ) suggesting its usefulness for validating XO-dependent contributions to  $\text{NO}_2^-$  reduction in biological systems. Combined, these data indicate care should be taken when choosing inhibition strategies as well as inhibitor concentrations when assigning relative  $\text{NO}_2^-$  reductase activity of AO and XOR.

© 2014 Elsevier Inc. All rights reserved.

\*Corresponding author at: University of Pittsburgh School of Medicine, Department of Anesthesiology, W1357 BST, 200 Lothrop Street, Pittsburgh, PA 15213, United States. Fax: +1 412 648 9587. ekelley@pitt.edu (E.E. Kelley).

<sup>1</sup>These authors contributed equally to this study.

## Keywords

Aldehyde oxidase; Nitrite; Xanthine oxidoreductase; Raloxifene; Nitric oxide; Febuxostat

---

## Introduction

Sources of nitric oxide alternative to the enzymatic activity nitric oxide synthases are currently being investigated as mediators of vascular function under hypoxic/inflammatory conditions. As a result, it has become apparent that inorganic nitrite ( $\text{NO}_2^-$ ) can serve as a robust reservoir of  $\cdot\text{NO}$  where hypoxia and acidic pH facilitate both non-enzymatic and enzymatic processes that reduce  $\text{NO}_2^-$  to  $\cdot\text{NO}$  [1,2]. One of the critical enzymatic processes reported to perform this  $\text{NO}_2^-$  reductase activity has been assigned to the molybdopterin family of enzymes; more specifically xanthine oxidoreductase (XOR) and aldehyde oxidase AO (AO), although other family members are currently under investigation. Recent reports have demonstrated  $\text{NO}_2^-$  reductase activity for both XOR and AO where  $\text{NO}_2^-$  is reduced by one electron to  $\cdot\text{NO}$  at the Mo-cofactor (Mo-co) when reducing equivalents are supplied directly to the Mo-co by hypo/xanthine (XOR) and/or aldehydes (AO) or indirectly via reduction of their respective FAD-cofactors by NADH [3–7]. This  $\text{NO}_2^-$  reductase activity is inhibited by  $\text{O}_2$  and thus optimally operative under low  $\text{O}_2$  tensions. Details regarding the micro-environmental factors influencing  $\cdot\text{NO}$  production capacity from XOR and AO have been recently reviewed in this journal [8].

Several tissues express abundant XOR as well as AO activity including the liver, intestine and lung. Therefore, assigning relative contributions of XOR and AO to  $\text{NO}_2^-$  – dependent  $\cdot\text{NO}$  formation necessitates either specific inhibition strategies or validation that the tissue in question does not express XOR or AO protein and/or activity. For the former, no commercially available antibodies exist that can distinguish between XOR and AO due to significant sequence homology (86%) between the two enzymes. For the later, both XOR and AO demonstrate a significant degree of promiscuity for substrates at their Mo-co active site. Adding to the frustration, XOR tissue-specific conditional knockouts are currently not available while global XOR<sup>-/-</sup> and XOR<sup>+/-</sup> mice experience alterations in nutrient absorption and elevated plasma hypoxanthine levels resulting in death from kidney failure before 6 weeks of age [9,10]. As for AO, there is only one report demonstrating successful knockout of one homologue of AO (aldehyde oxidase homologue 2, *Aoh2*) expressed primarily in the epithelium [11]. The current absence of knockout strategies to interrogate these molybdopterin enzymes has relegated investigators to employ pharmacologic means to conduct proof of principle experimentation regarding contributory roles mediating the effects of  $\text{NO}_2^-$  treatment. This being said, inhibitors of the Mo-co may also display overlap where-by an XOR inhibitor may partially inhibit AO or *vice versa*; especially when utilizing higher inhibitor concentrations. Recently, Uloric<sup>®</sup> (febuxostat) has been identified as a potent XOR-specific inhibitor ( $K_i = 0.96$  nM) [12]. Likewise, the estrogen receptor antagonist, raloxifene has been distinguished as a potent AO inhibitor ( $K_i = 1.0$  nM) [13]. These inhibitory characteristics have led investigators to use raloxifene and febuxostat to distinguish AO-dependent  $\text{NO}_2^-$  reduction from that mediated by XOR. While this approach

seems appropriate, the absence of cross-over inhibition analysis with both enzymes is problematic. Herein, we characterize the inhibition properties of raloxifene for XO and febuxostat for AO in order to more clearly define an approach with optimal potential for success.

## Materials and methods

### Materials

Xanthine, raloxifene, allopurinol, sodium nitrite, and menadione were from Sigma (USA). Xanthine oxidase (XO) was from Calbiochem (USA). Heparin Sepharose 6B Fast Flow (HS6B) was purchased from GE Healthcare (USA). Febuxostat was purchased from BIOTANG (USA). The  $\bullet$ NO donor 1-(hydroxy-NNO-azoxy)-L-proline (PROLI NONOate) and the electron paramagnetic resonance (EPR) spin trap 2-(4-carboxyphenyl)-4,5-dihydro-4,4,5,5-tetramethyl-1H-imidazolyl-1-oxy-3-oxide (cPTIO) were purchased from Cayman (USA).

### Nitric oxide measurement

Nitric oxide concentrations were verified using enhanced chemiluminescence with a Sievers Model 280 Nitric Oxide Analyzer (Boulder, CO). Authentication of  $\bullet$ NO as the species responsible for the observed signal was accomplished using cPTIO while positive controls were conducted with PROLI NONOate.

### XOR activity

Crystallized xanthine oxidase was further purified to remove ammonium sulfate using G25 Sephadex columns (GE Health Sciences, USA) and enzymatic activity determined by the rate of uric acid formation monitored ( $\lambda = 292$  nm) in potassium phosphate buffer (KPi) pH = 7.4. Units of activity are defined as: 1 Unit = 1  $\mu$ mole uric acid/min.

### XOR binding to heparin-Sepharose 6B (HS6B)

Purified XO was bound to HS6B as we previously described [14]. HS6B-XO was used by adding 100  $\mu$ L of XO (75 mUnits/mL in pH 7.4) to the purging vessel of the Nitric Oxide Analyzer containing 5 mL of KPi pH 6.5. Thus, the final working concentration of HS6B-XO activity was 1.5 mUnits/mL.

### Aldehyde oxidase

Incubations were performed using a technique previously described by Barr and Jones [15]. Briefly, incubation mixtures consisted of N-[2-(dimethylamino)ethyl]acridine-4-carboxamide (DACA, 6  $\mu$ M in DMSO), febuxostat (50–1000  $\mu$ M in DMSO), 25 mM potassium phosphate buffer with 0.1 mM EDTA (pH 7.4) in a final reaction volume of 800  $\mu$ L. Reactions were initiated by addition of human liver cytosol (HLC) to achieve a final concentration of 0.05 mg protein/mL. The final DMSO concentration in assay was 1% (v/v), which has no effect on the reaction [16]. Reactions were allowed to proceed for 5 min at 37  $^{\circ}$ C and subsequently quenched with 200  $\mu$ L of 1.0 M formic acid containing a known concentration of 2-methyl-4( $^3$ H)-quinazolinone as internal standard. Quenched samples

were centrifuged at 5000 rpm for 10 min in a 5415D Eppendorf centrifuge and the supernatant collected for analysis by LC–MS/MS [15].

## Statistics

Data were analyzed using one way analysis of variance followed by Tukey's range test for multiple pair-wise comparisons. Significance was determined as  $p < 0.05$ .

## Results

Purified xanthine oxidase was exposed to various concentrations of raloxifene (0–100  $\mu\text{M}$ ) in the presence of xanthine (100  $\mu\text{M}$ ) and monitored for uric acid formation, Fig. 1A. Raloxifene inhibited XO-catalyzed xanthine oxidation to uric acid in a concentration-dependent manner achieving complete inhibition near 100  $\mu\text{M}$ . Inhibition of XO with allopurinol is also shown for comparison. Plotting the inverse of initial reaction velocity ( $1/V_0$ ) versus the concentration of inhibitor (Dixon Plot) revealed a competitive inhibition process with a  $K_i = 13 \mu\text{M}$  for raloxifene, Fig. 1B. Examination of the effects of pH (5.5–9) on inhibition strength demonstrated greater potency for raloxifene at lower pH; values similar to those encountered *in vivo* under hypoxia/inflammation, Fig. 1C. The time to inhibition was found to be rapid with no observable difference between 0 and 60 s, Fig 1D.

To assess the capacity of raloxifene to inhibit XO-catalyzed  $\text{NO}_2^-$  reduction to  $\cdot\text{NO}$ , purified XO was bound to heparin-Sepharose 6B beads (HS6B-XO) and added to the reaction chamber of the Nitric Oxide Analyzer containing 1 mM  $\text{NO}_2^-$  and 20  $\mu\text{M}$  xanthine as depicted in Fig. 2A. Immobilization of XO on artificial glycosaminoglycans (GAGs) such as HS6B facilitates  $\text{NO}_2^-$  reductase activity and serves to protect the enzyme from degradation induced by the physical action of the flow-through purging process. After attainment of a rate of  $\cdot\text{NO}$  formation, the inhibitor was added and measurements were taken. Results for raloxifene, menadione, and the XO-specific inhibitor febuxostat are plotted as percent inhibition versus inhibitor concentration, Fig 2B. These data produced  $\text{EC}_{50}$  values as follows: raloxifene (64  $\mu\text{M}$ ), menadione (60 nM), and febuxostat (4 nM). Experiments using 100–500  $\mu\text{M}$   $\text{NO}_2^-$  produced similar results but with greater variability and diminished window of opportunity for observing signal diminution by inhibition (not shown). Experiments whereby HS6B-XO was exposed to the inhibitor before reaction initiation produced similar results (not shown). Control experiments where either the inhibitor or DMSO (solvent for inhibitors) was exposed to decaying PROLI NONOate produced no observable diminution of signal indicating the absence of direct actions between inhibitor/solvent and  $\cdot\text{NO}$ .

To examine potential inhibitory actions of febuxostat for AO, human liver cytosol was exposed to various concentrations of febuxostat and assessed for using 6  $\mu\text{M}$  of the AO selective substrate N-[2-(dimethylamino)ethyl]acridone-4-carboxamide (DACA) [15], Fig. 3. Plotting percent inhibition versus febuxostat concentration revealed an  $\text{IC}_{50}$  of 613  $\mu\text{M}$  with complete inhibition occurring at levels over 1 mM.

## Discussion

The potential therapeutic impact of  $\text{NO}_2^-$ -mediated enhancement of  $\bullet\text{NO}$  bioavailability is evolving rapidly as reports of salutary actions of  $\text{NO}_2^-$  treatment are appearing at steady rate. As such, understanding the reductive processes driving this alternative  $\bullet\text{NO}$  pathway is vital. The molybdopterin-containing enzymes XO and AO have been identified as potential contributors to this pathway by demonstrating  $\text{NO}_2^-$  reductase activity under conditions similar to those that diminish the  $\bullet\text{NO}$  production capacity of nitric oxide synthase; hypoxia and acidic pH. However, as stated above, several factors coalesce to provide significant obstacles to successfully assigning relative contributions to  $\bullet\text{NO}$  formation to AO and XO in cell and tissue systems affirming the need for a more viable approach.

Previous reports have indicated potent inhibition ( $K_i = 1.0\text{--}51$  nM, depending on the reducing substrate) properties of raloxifene for AO and thus this compound has been used to explore AO-mediated biochemistry including  $\text{NO}_2^-$  reduction [4,13,16]. However, there exists no detailed analysis regarding crossover inhibition of XO by raloxifene. Herein, we tested raloxifene for capacity to inhibit XO-catalyzed xanthine oxidation to uric acid and found significant inhibition ( $K_i = 13$   $\mu\text{M}$ ) suggesting that application of raloxifene to specifically inhibit AO at concentrations near this level would induce considerable inhibition of XO. In addition, inhibition of XO by raloxifene was more pronounced under slightly acidic conditions similar those encountered in a hypoxic/inflammatory milieu. More importantly, it was determined that raloxifene inhibits XO-catalyzed  $\text{NO}_2^-$  reduction with albeit less potency ( $\text{EC}_{50} = 64$   $\mu\text{M}$ ) than that observed for xanthine oxidation to uric acid. However, inhibition of XO-dependent  $\text{NO}_2^-$  reduction was not observed below  $1.0$   $\mu\text{M}$  suggesting that application of raloxifene at concentrations up to  $1.0$   $\mu\text{M}$  would serve to completely inhibit AO while not altering XO-catalyzed reactions. It is important to note that menadione, a commonly used alternative to raloxifene for AO inhibition analysis, did not alter XO-mediated uric acid oxidation; yet, it did potently inhibit XO-catalyzed  $\text{NO}_2^-$  reduction to  $\bullet\text{NO}$  ( $\text{EC}_{50} = 60$  nM) [17,18]. It is also crucial to note that we are not endorsing the use of raloxifene for *in vivo* studies as it is an estrogen receptor antagonist and thus not an AO-specific inhibitor.

Combined, these data suggest that application of raloxifene at sub- $\bullet\text{M}$  concentrations is an appropriate strategy for discerning AO-catalyzed  $\text{NO}_2^-$  reduction from that mediated by XOR in cell culture and *ex vivo* tissue experimentation whereas the use of menadione should be avoided.

Febuxostat (Uloric<sup>®</sup>) has been identified as an XOR-specific inhibitor that: (1) is 3 orders of magnitude more potent than the classical pyrazalopyrimidine-based XO inhibitor allopurinol ( $K_i = 0.96$  nM vs.  $0.7$   $\mu\text{M}$ ) and (2) unlike allo/oxy purinol, is not affected by XO-endothelial GAG interactions and does not affect alternative purine catabolic pathways [12,19]. However, there have been no reports investigating potential inhibitory action of febuxostat on AO. Herein, we report febuxostat to be a superior inhibitor of XO-catalyzed  $\text{NO}_2^-$  reduction ( $\text{EC}_{50} = 4$  nM) while demonstrating very poor inhibition properties for AO ( $\text{EC}_{50} = 613$   $\mu\text{M}$ ). In addition, our previous studies revealed no interaction between DACA and XO

affirming no interference of XO catalyzed reactions and DACA catabolism [20]. These data suggest that application of febuxostat to specifically inhibit XO-catalyzed  $\text{NO}_2^-$  reduction would be an appropriate approach as febuxostat is not only superior to allopurinol but does not alter AO Mo-co-catalyzed reactions.

*In toto*, limitations including the absence of genetic knockout models have relegated investigators to employ pharmacologic means to distinguish between XOR- and AO-catalyzed reactions. Of developing importance is the capacity to distinguish between XOR- and AO-catalyzed reduction of  $\text{NO}_2^-$  to  $\cdot\text{NO}$  in cell culture and tissues. Herein, we report that sub- $\mu\text{M}$  concentrations of raloxifene will serve to specifically inhibit AO while concentrations of febuxostat below 100  $\mu\text{M}$  will specifically inhibit XOR in the absence of either inhibitor participating in observable crossover inhibition.

## Acknowledgments

This work was supported by a National AHA Scientist Development Grant 10SDG3560005 and University of Pittsburgh, Department of Anesthesiology Development Grant (EEK) and by the National Institutes of Health, National Institute of General Medical Sciences [Grant GM100874] (J.P.J.).

## Abbreviations

<b>AO</b>	aldehyde oxidase
<b>GAGs</b>	glycosaminoglycans
<b>H<sub>2</sub>O<sub>2</sub></b>	hydrogen peroxide
<b><math>\cdot\text{NO}</math></b>	nitric oxide
<b>NOS</b>	nitric oxide synthase
<b>O<sub>2</sub><sup>-</sup></b>	superoxide
<b>RNS</b>	reactive nitrogen species
<b>ROS</b>	reactive oxygen species
<b>XDH</b>	xanthine dehydrogenase
<b>XO</b>	xanthine oxidase
<b>XOR</b>	xanthine oxidoreductase

## References

1. Gladwin MT. Evidence mounts that nitrite contributes to hypoxic vasodilation in the human circulation. *Circulation*. 2008; 117:594–597. [PubMed: 18250278]
2. Lundberg JO, Carlstrom M, Larsen FJ, Weitzberg E. Roles of dietary inorganic nitrate in cardiovascular health and disease. *Cardiovasc Res*. 2011; 89:525–532. [PubMed: 20937740]
3. Millar TM, Stevens CR, Benjamin N, Eisenthal R, Harrison R, Blake DR. Xanthine oxidoreductase catalyses the reduction of nitrates and nitrite to nitric oxide under hypoxic conditions. *FEBS Lett*. 1998; 427:225–228. [PubMed: 9607316]
4. Li H, Kundu TK, Zweier JL. Characterization of the magnitude and mechanism of aldehyde oxidase-mediated nitric oxide production from nitrite. *J Biol Chem*. 2009; 284:33850–33858. [PubMed: 19801639]

5. Li H, Cui H, Kundu TK, Alzawahra W, Zweier JL. Nitric oxide production from nitrite occurs primarily in tissues not in the blood: critical role of xanthine oxidase and aldehyde oxidase. *J Biol Chem.* 2008; 283:17855–17863. [PubMed: 18424432]
6. Li H, Samouilov A, Liu X, Zweier JL. Characterization of the magnitude and kinetics of xanthine oxidase-catalyzed nitrite reduction. Evaluation of its role in nitric oxide generation in anoxic tissues. *J Biol Chem.* 2001; 276:24482–24489. [PubMed: 11312267]
7. Huang L, Borniquel S, Lundberg JO. Enhanced xanthine oxidoreductase expression and tissue nitrate reduction in germ free mice. *Nitric Oxide.* 2010; 22:191–195. [PubMed: 20142047]
8. Cantu-Medellin N, Kelley EE. Xanthine oxidoreductase-catalyzed reduction of nitrite to nitric oxide: insights regarding where, when and how. *Nitric Oxide.* 2013; 34:19–26. [PubMed: 23454592]
9. Vorbach C, Scriven A, Capecchi MR. The housekeeping gene xanthine oxidoreductase is necessary for milk fat droplet enveloping and secretion: gene sharing in the lactating mammary gland. *Genes Dev.* 2002; 16:3223–3235. [PubMed: 12502743]
10. Ohtsubo T, Rovira II, Starost MF, Liu C, Finkel T. Xanthine oxidoreductase is an endogenous regulator of cyclooxygenase-2. *Circ Res.* 2004; 95:1118–1124. [PubMed: 15528468]
11. Terao M, Kurosaki M, Barzago MM, Fratelli M, Bagnati R, Bastone A, Giudice C, Scanziani E, Mancuso A, Tiveron C, Garattini E. Role of the molybdoflavoenzyme aldehyde oxidase homolog 2 in the biosynthesis of retinoic acid: generation and characterization of a knockout mouse. *Mol Cell Biol.* 2009; 29:357–377. [PubMed: 18981221]
12. Malik UZ, Hundley NJ, Romero G, Radi R, Freeman BA, Tarpey MM, Kelley EE. Febuxostat inhibition of endothelial-bound XO: implications for targeting vascular ROS production. *Free Radical Biol Med.* 2011; 51:179–184. [PubMed: 21554948]
13. Obach RS. Potent inhibition of human liver aldehyde oxidase by raloxifene. *Drug Metab Dispos.* 2004; 32:89–97. [PubMed: 14709625]
14. Kelley EE, Trostchansky A, Rubbo H, Freeman BA, Radi R, Tarpey MM. Binding of xanthine oxidase to glycosaminoglycans limits inhibition by oxypurinol. *J Biol Chem.* 2004; 279:37231–37234. [PubMed: 15231841]
15. Barr JT, Jones JP. Evidence for substrate-dependent inhibition profiles for human liver aldehyde oxidase. *Drug Metab Dispos.* 2013; 41:24–29. [PubMed: 22996261]
16. Choughule KV, Barr JT, Jones JP. Evaluation of rhesus monkey and guinea pig hepatic cytosol fractions as models for human aldehyde oxidase. *Drug Metab Dispos.* 2013; 41:1852–1858. [PubMed: 23918666]
17. Obach RS, Huynh P, Allen MC, Beedham C. Human liver aldehyde oxidase: inhibition by 239 drugs. *J Clin Pharmacol.* 2004; 44:7–19. [PubMed: 14681337]
18. Johns DG. Human liver aldehyde oxidase: differential inhibition of oxidation of charged and uncharged substrates. *J Clin Invest.* 1967; 46:1492–1505. [PubMed: 4226961]
19. Takano Y, Hase-Aoki K, Horiuchi H, Zhao L, Kasahara Y, Kondo S, Becker MA. Selectivity of febuxostat, a novel non-purine inhibitor of xanthine oxidase/xanthine dehydrogenase. *Life Sci.* 2005; 76:1835–1847. [PubMed: 15698861]
20. Barr JT, Jones JP. Evidence for substrate-dependent inhibition profiles for human liver aldehyde oxidase. *Drug Metab Dispos.* 2013; 41:24–29. [PubMed: 22996261]

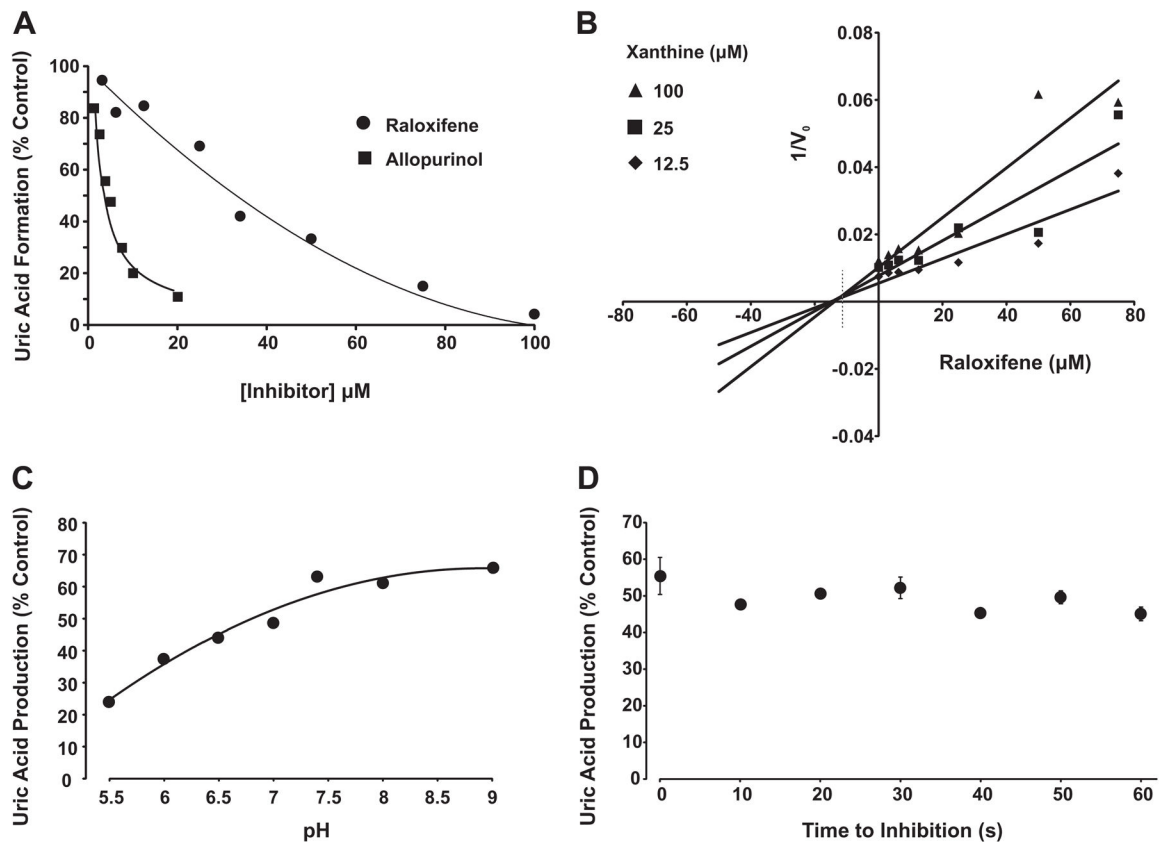


**Fig. 1.**

Raloxifene inhibition of XO. (A) Purified xanthine oxidase (2 mUnits/ml, phosphate buffered saline, pH 7.4) was exposed to various concentrations of either raloxifene or allopurinol and assessed for formation uric acid ( $\lambda = 295$  nm) upon the addition of xanthine (100  $\mu$ M). Shown are the initial reaction rates ( $V_0$ ) plotted as % control (no inhibitor). (B) Purified xanthine oxidase (as above) was exposed to various concentrations of raloxifene and assessed for formation uric acid ( $\lambda = 295$ ) using 3 concentrations of xanthine (12.5, 25, and 100  $\mu$ M). Shown is a Dixon plot ( $1/V_0$  vs. [inhibitor]) generating an inhibition constant ( $K_i$ ) = 13  $\mu$ M for raloxifene and demonstrating a competitive inhibition process defined as line intersection above the abscissa (*dashed line*). (C) Purified xanthine oxidase (as above) was exposed to a single concentration of raloxifene (37  $\mu$ M) and assessed for the effect of pH (5.5–9.0) on inhibition capacity. (D) Purified xanthine oxidase (as above) was exposed to a single concentration of raloxifene (37  $\mu$ M) and assessed for time to inhibition (0–60 s). For (A–C), data represent the mean of at least 4 independent determinations. For (D), data represent the mean and standard deviation of at least 3 independent determinations with no significant difference observed at 95% confidence,  $p > 0.05$ .



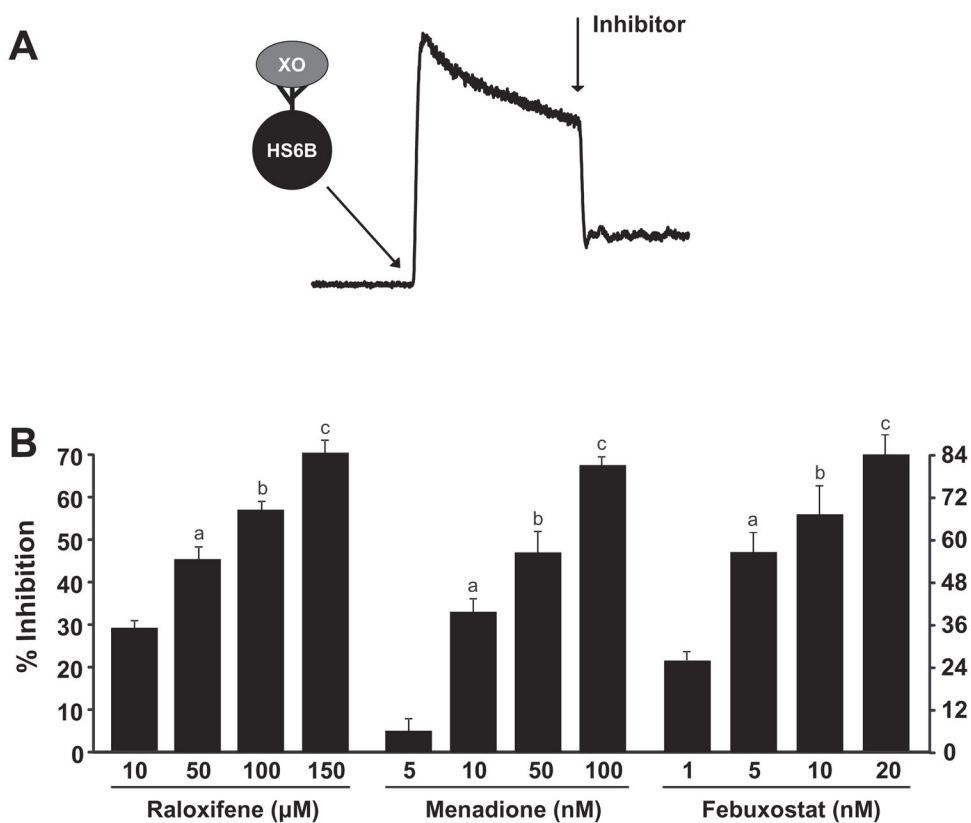


**Fig. 2.**

Inhibition of XO-catalyzed  $\text{NO}_2^-$  reduction to  $\cdot\text{NO}$ . (A) Diagram depicting a typical experiment where HS6B-XO (final concentration = 1.5 mUnits/mL) was added to the reaction vessel of the Nitric Oxide Analyzer containing 1 mM  $\text{NaNO}_2^-$  and 20  $\mu\text{M}$  xanthine. After establishment of a rate of  $\cdot\text{NO}$  generation, the inhibitor was added. All inhibitors were added at the same time after the addition of HS6B-XO (B) Inhibition profiles for raloxifene, menadione, and febuxostat generating  $\text{EC}_{50}$  values of 64  $\mu\text{M}$ , 60 nM and 4 nM, respectively. For raloxifene a–c are significantly different from 10  $\mu\text{M}$  as well as between groups  $p < 0.05$ . For menadione a–c are significantly different from 5 nM as well as between groups  $p < 0.05$ . For febuxostat, a–c are significantly different from 1.0 nM,  $p < 0.05$  and a is significantly different from c,  $p < 0.05$ .

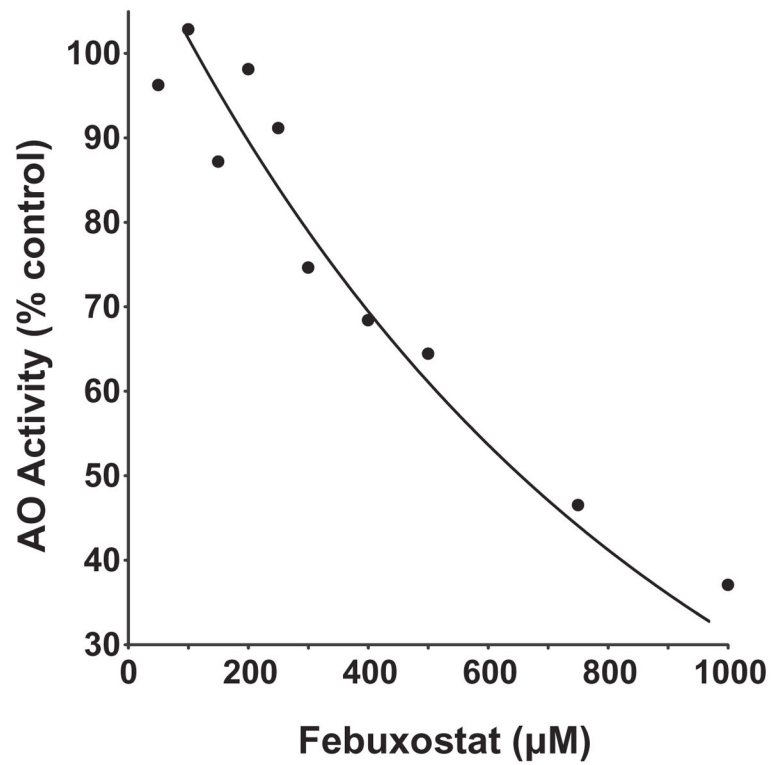


**Fig. 3.** Febuxostat inhibition of AO. The fractional inhibition of the AO-specific substrate DACA in human liver cytosol (0.05 mg protein/ml) exposed to various concentrations of febuxostat (0–1 mM). The DACA concentration was fixed at 6 µM and reaction progress determined by LC–MS/MS. The IC<sub>50</sub> for febuxostat inhibition of DACA metabolism was determined to be 613 µM. Data represent the mean of at least 3 independent determinations.